Eur. Phys. J. D **38**, 3–13 (2006)
DOI: 10.1140/epjd/e2006-00027-1

THE EUROPEAN PHYSICAL JOURNAL D

# Chemical stereodynamics: retrospect and prospect

D. Herschbach[a]

Department of Chemistry and Chemical Biology, Harvard University, 12 Oxford Street, Cambridge, Massachusetts 02138, USA
and
Department of Physics, Texas A & M University, College Station, Texas 77843-4242, USA

Received 8 December 2005
Published online 8 February 2006 – 

**Abstract.** Thematic aspects of chemical stereodynamics are discussed that offer much scope for further development. Particularly emphasized are opportunities to exploit angular correlations to recover information usually presumed to be inaccessible; means to hybridize rotational angular momentum and thereby create spatially oriented or aligned pendular states in which molecular axes are confined to oscillate about the direction of an external field; the major role of atomic electronegativity differences in producing steric preferences in reactivity, by affecting the location of nodes and asymmetric composition in molecular orbitals; and some newly recognized stereodynamic aspects of DNA replication.

**PACS.** 33.15.Bh General molecular conformation and symmetry; stereochemistry – 31.10.+z Theory of electronic structure, electronic transitions, and chemical binding – 83.37.-j Single molecule kinetics

## 1 Introduction

The Osaka conference served admirably to survey the burgeoning scope of chemical stereodynamics and to assess prospects. In this paper, my chief aim is to revisit, from my emeritus perspective, four thematic aspects that underlie much current work and invite further development. These illustrate: (1) How to recover seemingly "forbidden fruit", information obscured either by uncontrollable initial conditions or proscribed by quantum mechanics. (2) How to "bring molecules to attention", by subduing the random spatial orientations imposed by rotational tumbling. This capability has been exploited in numerous ways, now including tomographic imaging of electron distributions in molecular orbitals. (3) How to interpret, in terms of electronic properties, the steric preferences found for few-body reactions in single-collision experiments and thereby likely gain heuristic insights applicable to a much wider chemical domain. (4) How rudimentary stereodynamic ideas find use in new contexts. This is exemplified by a recent reinterpretation of optical-tweezer experiments, employing the venerable Langevin-Debye formula to model the dependence on tension of enzyme-catalyzed DNA replication rates.

As a prologue, we should offer homage to some ancestral scientists [1]. In the early 19th century, Hashimoto, a physician from Osaka, pursued extensive studies of electricity. He strived to understand how static electricity was produced by friction (a process involving directional stroking!) and elucidated some aspects of lightning. He constructed an electrostatic generator ("Erekitera") and published in 1811 a book presenting "physical principles of electricity", urging readers to try experiments of their own. Another notable scientist, Nagaoka, in 1931 became the first president of Osaka Imperial University. He had studied in Berlin as well as Tokyo, conducted experiments on magnetostriction, and in 1904 proposed a prescient atomic model. In analogy to the planet Saturn, his model postulated a large positively charged core encircled by a ring of much lighter negatively charged particles. Rutherford, in describing his discovery of the nucleus in 1911, cited Nagaoka's model. Surely, it deserves credit as an antecedent to the celebrated model proposed by Bohr in 1913. Nagaoka went on to study atomic emission spectra of more than 30 elements, ranging from hydrogen to uranium!

Another historical homage is apt for any discussion of directional properties of atomic and molecular collisional or spectroscopic processes. Many aspects stem from the demonstration of space quantization in 1922 by Stern and Gerlach [2]. Their work, the ancestor of myriad molecular beam experiments and much else, including laser spectroscopy, was recently commemorated in a fitting way by naming in their honor a new center for experimental physics at the University of Frankfurt.

## 2 Pursuit of forbidden fruit

As Otto Stern liked to emphasize, the great appeal of the molecular beam method is its conceptual simplicity and directness. However, no matter how much care is devoted to defining or analyzing directions, velocities, and internal states of the collision partners, the dynamical resolution of

[a] e-mail: dherschbach@yahoo.com

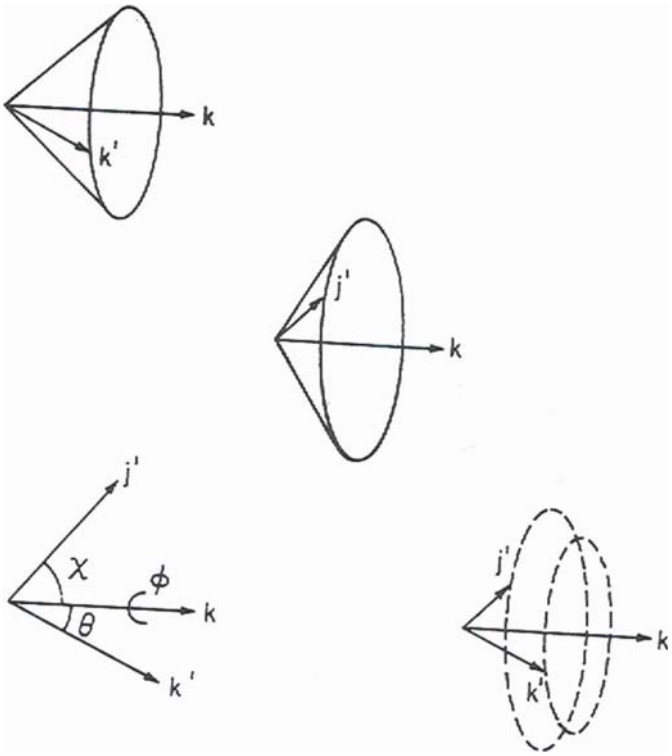


**Fig. 1.** Three-vector correlation among initial and final relative velocity vectors, denoted by $\mathbf{k}$ and $\mathbf{k}'$, and product rotational angular momentum vector $\mathbf{j}'$. Upper pair of diagrams indicate the azimuthal symmetry about $\mathbf{k}$ of the $\mathbf{k}'$ and $\mathbf{j}'$ vectors, inherent when these are observed separately, as in the two-vector correlations ($\mathbf{k}$, $\mathbf{k}'$) and ($\mathbf{k}$, $\mathbf{j}'$). Lower pair of diagrams indicates how the three-vector correlation ($\mathbf{k}$, $\mathbf{k}'$, $\mathbf{j}'$) can give information about the dihedral angle $\phi$, in effect undoing the azimuthal averaging about the initial relative velocity.

beam scattering experiments is limited by random aspects of the initial conditions. Even if the reactant molecules are oriented, there remains the "dartboard" distribution of impact parameters in the collision. Dynamical information obscured by averaging over the random orientations of impact parameters was long thought to be irretrievable.

### 2.1 Undoing azimuthal averaging

Yet in principle and in practice such "forbidden fruit" can be harvested [3]. Figure 1 indicates how the averaging over impact parameter can be undone [4–6]. The random azimuthal distribution of impact parameters makes the final relative velocity vector $\mathbf{k}'$ and product rotational angular momentum $\mathbf{j}'$ (or any other product vector property) azimuthally symmetric about the initial relative velocity vector $\mathbf{k}$. The forces acting in the collision do not usually have such symmetry (unless both partners are spherical). In the same way, darts thrown at a board exhibit azimuthal symmetry even when the thrower has astigmatism.

The redeeming strategy is to measure two product vectors such as $\mathbf{k}'$ and $\mathbf{j}'$ simultaneously and thereby to determine the *three-vector correlation* among $\mathbf{k}$, $\mathbf{k}'$, and $\mathbf{j}'$. When a subset is selected of $\mathbf{k}'$ vectors with particular $\mathbf{j}'$ (or vice versa), this subset in general will not have azimuthal symmetry about $\mathbf{k}$. Accordingly, the dihedral angle $\phi$ between the ($\mathbf{k}$, $\mathbf{k}'$)- and ($\mathbf{k}$, $\mathbf{j}'$)-planes need not be uniformly distributed. Evaluating the distribution of $\phi$ recoups information about the reaction dynamics that otherwise would be lost by the azimuthal average over impact parameters.

As a chemical analogy, consider a helium atom in its ground state. The distribution of each electron, viewed separately, is spherically symmetric. But if the two electrons are observed simultaneously, their positions are strongly correlated as a consequence of their repulsive interaction. If not known beforehand, the presence of this repulsion would be revealed by the simultaneous observation, although not by viewing the electrons singly.

Although it is convenient to use the product rotational angular momentum $\mathbf{j}'$ as the "extra" quantity in the three-vector correlation, this poses an instructive question. According to quantum mechanics, only the magnitude and one projection of an angular momentum vector can be specified. Since we envision a measurement that specifies both the magnitude of $\mathbf{j}'$ and the polar angle $\chi$ between $\mathbf{j}'$ and $\mathbf{k}$, the azimuthal angle about $\mathbf{k}$ should be unobservable. Is not the dihedral angle $\phi$ therefore unobservable after all? That is so, for any particular measurement. But this can be circumvented by measuring the angular momentum distribution using several different choices for the axis of quantization. The data can then be combined to obtain moments of the $\phi$ distribution as well as those of $\chi$ and the scattering angle $\theta$ between the $\mathbf{k}$ and $\mathbf{k}'$ velocity vectors. The classical version of the three-vector correlation hence can be resurrected, including its $\phi$ dependence [4]. In this sense, quantum mechanics in effect allows a dihedral angle such as $\phi$ to be observed even when the uncertainty principle does not permit this in any particular measurement.

This undoing of impact parameter averaging in molecular collisions has some heuristic resemblance to the celebrated "phase problem" encountered in X-ray crystallography. Both are resolved by introducing additional observables that provide new reference points, and by combining data from variant experiments.

### 2.2 Prospects for vector correlations

The theory of angular correlations has proved very fruitful in the analysis of nuclear reactions [7]. It was thus natural to emulate that in the early days of chemical stereodynamics. My group focused on product vector correlations. Theoretical aspects we studied included statistical models for two-vector [8], three-vector [9], and four-vector [10, 11] angular correlations. Although many reactions exhibit markedly nonstatistical dynamics, the statistical models provide a useful reference for assessing the nonstatistical features, particularly by information theory methods [12]. We also developed impulsive dynamical models for both ($\mathbf{k}$, $\mathbf{k}'$) angular distributions [13] and for the ($\mathbf{k}$, $\mathbf{k}'$, $\mathbf{j}'$)

three-vector correlation [14], as well as trajectory calculations illustrating the use of the $\phi$-distribution as a diagnostic property [15].

Early crossed molecular beam experiments dealt almost solely with ($\mathbf{k}$, $\mathbf{k}'$) distributions, the most readily accessible. Later measurements of ($\mathbf{k}$, $\mathbf{j}'$) correlations were added, chiefly by deflecting polar product molecules in an electric field gradient (analogous to the Stern-Gerlach magnet). That technique also enabled a first study of the ($\mathbf{k}$, $\mathbf{k}'$, $\mathbf{j}'$) three-vector correlation [3]. This showed that in the Cs + $CH_3I$ reaction the CsI product $\mathbf{j}'$ was not azimuthally symmetric about $\mathbf{k}$ but rather was strongly aligned (preferred $\phi \sim 90°$), perpendicular to the plane containing $\mathbf{k}$ and $\mathbf{k}'$. The newly formed product molecule thus tends to rotate in the plane containing the initial asymptotic trajectories of the reactants and the final trajectories of the reactants. Model calculations soon confirmed such alignment is typical, weakly in the statistical regime [9] and more strongly when impulsive repulsion occurs between the reaction products [16].

An optimistic view of prospects for greatly enhanced experimental studies of vector correlations in chemical reactions appeared justified by these early results, in view of the vigorous development of laser spectroscopy of great sensitivity and resolution [17]. In anticipation of the ability to both select $\mathbf{j}$ and $\mathbf{k}$ and measure $\mathbf{j}'$ as well as $\mathbf{k}'$, it was even expected that the ($\mathbf{j}$, $\mathbf{k}$, $\mathbf{k}'$, $\mathbf{j}'$) four-vector correlation might become experimentally accessible. Since in principle state selection that distinguishes $\mathbf{j}$ from $-\mathbf{j}$ and measurements that distinguish $\mathbf{j}'$ from $-\mathbf{j}'$ can be made, the four-vector correlation can even determine the relative sense of rotation (parallel or contrary) of the reactant and product molecules, as well as undoing other angular averages implicit in lower order correlations [11].

The optimism proved to be quite premature. Over the past 30 years, experiments employing molecular beams and lasers have provided a host of further results for the ($\mathbf{k}$, $\mathbf{k}'$) and ($\mathbf{k}$, $\mathbf{j}'$) correlations. However, only one further ($\mathbf{k}$, $\mathbf{k}'$, $\mathbf{j}$) correlation has been reported [18]; in an elegant experiment, Zare and colleagues showed for HCl from the Cl + $CH_4$ reaction that the preferred dihedral angle is again $\phi \sim 90°$. Only one experiment pertaining to a ($\mathbf{j}$, $\mathbf{k}$, $\mathbf{k}'$, $\mathbf{j}'$) four-vector correlation has been reported [19]; this employed 2-color Doppler circular dichroism in a novel way.

This history may suggest that going beyond two-vector correlations is unduly challenging. Yet the "forbidden fruit" offered by those correlations is of fundamental value for stereodynamics. That has been further exemplified in recent theoretical studies, including detailed analysis of ($\mathbf{k}$, $\mathbf{k}'$, $\mathbf{j}'$) for the H + $D_2$ reaction [20,21] and an comprehensive treatment of angular correlations [22]. Also awaiting application is a detailed strategy for obtaining the maximum information about the angular correlations containing $\mathbf{j}'$ that can be extracted from resonance fluorescence measurements [23]. This involves combining data obtained with several distinct choices of the quantization axis. Not only a reference axis associated with the collision process but a plane must be established to observe a three-vector correlation, and two planes to observe a four-vector correlation. New experimental capabilities (some described below, in Sect. 3) likely can be adapted to such tasks. In my wistful view, the promise revealed by theory ought to spur experimentalists to rise to the challenge.

## 3 Bringing molecules to attention

In typical collisional or spectroscopic experiments, molecules are not only randomly oriented but rotate freely, imposing isotropic averaging of interactions. Hopes of avoiding this entropic curse have motivated many efforts to develop means to restrict molecular rotation, reviewed elsewhere [24]. Methods that produce alignment of rotational angular momentum have a long and virtuous history, both in bulk and beam experiments, but will not be considered here. Rather, our concern is with the ability to align or orient a molecular axis, as required for studies of the stereodynamics of gas phase collisions. Note that the anisotropy created by *alignment* behaves like a double-headed arrow ($\leftrightarrow$), and that created by *orientation* behaves like a single-headed arrow ($\rightarrow$).

### 3.1 Precessing, pinwheeling, and pendular molecules

In the mid-1960s, Bernstein and Brooks pioneered experiments with oriented symmetric top molecules, employing electric field focusing [25]. The method depends on the fact that symmetric tops in most rotational states (other than $K = 0$) precess rather than tumble. As a result, the dipole moment does not average out but rather has a constant projection on the local field direction, giving rise to a first-order Stark effect. State selection by the focusing field thus suffices to pick out molecules with substantial intrinsic orientation of the figure axis. This is an excellent method; it has enabled incisive studies of "head vs. tail" reaction probabilities in collisions with both gas molecules and surfaces. However, besides its limitation to symmetric tops, the method requires somewhat elaborate apparatus.

Orientation of polar molecules other than symmetric tops by an electric field was long considered to be quite impractical [17]. The rotational tumbling of diatomic, linear, or asymmetric top molecules averages out the dipole moment in first order and hence greatly weakens interaction with an electric field. Curiously, although the drastic cooling of rotation attainable in supersonic molecular beams had been well understood much earlier, it was only in the 1990s that this was exploited to make feasible molecular orientation and alignment, by Loesch at Bielefeld [26] and in our laboratory at Harvard [27]. When the rotational energy is low enough, molecular pinwheeling can be quenched without use of an inordinately high field strength. The molecular axis then remains confined to a restricted range, as it swings to and fro about the field direction, like a pendulum.

Such pendular states are readily created for either polar or paramagnetic molecules, and for linear or asymmetric rotors as well as symmetric tops. In the presence of

the field, the eigenstates become coherent linear superpositions or hybrids of the field-free rotational states. These hybrids coincide with the familiar second-order Stark or Zeeman states when the dipole and/or the moment of inertia is small or the field is weak; then the molecule continues to tumble like a pinwheel. When the interaction is sufficiently strong, however, the hybrids become pendular. The magnetic version produces alignment rather than orientation, but is applicable to many molecules not accessible to the electric version; this includes paramagnetic nonpolar molecules and molecular ions (which would just crash into an electrode if subjected to an electric field). The experimental simplification is major because a focusing field (typically a meter long and expensive to fabricate) is not needed. Instead, the molecular beam is merely sent between the plates of a small condenser (usually about 1 $cm^2$ in area and a few mm apart) or between the pole pieces of a compact magnet. The uniform field which creates the hybrid eigenstates need extend over the small region in which the beam actually interacts with its target.

A kindred variety of pendular states can be obtained by utilizing the induced dipole moment created by nonresonant interaction of intense laser radiation with the molecular polarizability [28]. This can produce alignment whether the molecule is polar, paramagnetic, or neither, as long as the polarizability is anisotropic. That is generally the case; e.g. for a linear molecule the polarizability is typically about twice as large along the axis as transverse to it. Although the electric field of the laser rapidly switches direction, since the interaction with the induced dipole is governed by the square of the field strength, the direction of the aligning force experienced by the molecule remains the same. With a pulsed laser, the field strength can readily be made high enough to attain strong alignment.

The polarizability anisotropy does not distinguish between the two ends of a molecule, whether or not they differ. Therefore, as indicated in Figure 2, even for a heteropolar molecule such as ICl the induced dipole is the same in both directions and the interaction with the laser creates a symmetric double-well potential. The energy levels associated with the pendular motion of an aligned molecule thus are split by tunneling between the two potential wells. The tunneling rate can be varied over many orders of magnitude by scanning the laser intensity over a modest range [29]. In many cases, the tunneling splitting will be very small for the lowest pair of pendular energy levels. If the molecule is polar, introducing in addition a static electric field, congruent with the laser field, connects the nearly degenerate tunneling doublets, which have opposite parity. Even a weak static field can thus produce a strong pseudo-first-order Stark effect. Almost any polar molecule, linear or asymmetric, can thereby be made to act like a symmetric top for the duration of the laser pulse [30].

Of special interest is the possibility of aligning or orienting molecules with respect to more than one lab-fixed axis. This could be done by a static field orienting a permanent dipole moment while a linearly polarized laser field aligns an induced dipole perpendicular to the permanent moment. A more elegant method, recently demonstrated, uses an intense, elliptically polarized laser field to simultaneously align all three principal axes of a molecule [31], thereby exploiting fully the anisotropy of the polarizability tensor.

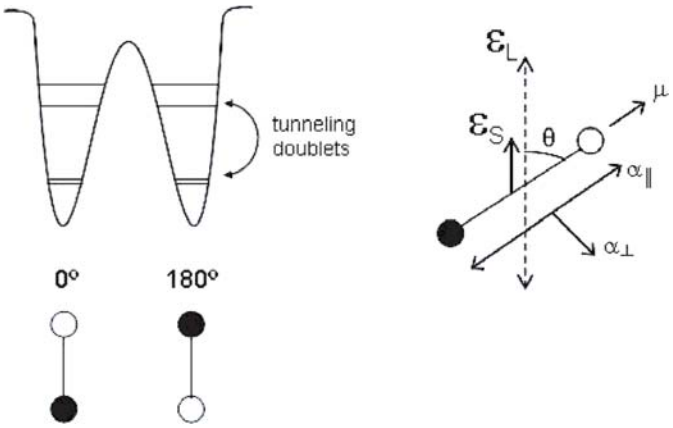


**Fig. 2.** Right: schematic depicting interaction of a polar diatomic molecule with a strong electric field, $E_L$, produced by nonresonant laser light, and a weak, collinear static field, $E_S$. The molecular axis is at an angle $\theta$ with respect to the field vectors. The rapid reversal in direction of $E_L$ averages out its interaction with the permanent dipole moment, $\mu$, whereas the induced dipole resulting from the anisotropy of the molecular polarizability, $\Delta\alpha = \alpha_{||} - \alpha_\perp$, does not average out because the interaction is proportional to $E_L^2$. Left: double-well potential produced by the induced dipole interaction, proportional to $\cos^2\theta$. The intervening barrier height is proportional to $\Delta\alpha E_L^2$ and to the moment of inertia. If the barrier is high enough, the lowest pair of pendular states will be nearly degenerate in energy, only slightly split by tunneling through the barrier. When a static field is present, the nearly degenerate pair of states is connected by a perturbation, proportional to $\mu E_S \cos\theta$, so the energy levels split apart strongly, producing a first-order Stark effect.

Typically, for the varieties of pendular states thus far noted, the coherent hybrid eigenstates form adiabatically as they traverse the field region. Outside the field, however, the orientation or alignment rapidly disappears. Although many experiments can be done in the presence of the external field, others cannot. In such cases, it may be feasible to obtain nonadiabatic alignment. This is done by use of a suitable nonresonant laser pulse to produce a rotational wavepacket. After the molecule departs the field, the rotational packet will periodically rephase, giving recurrent alignment of the molecular axis [32]. This technique, providing alignment in the absence of an external field, is serviceable whenever the experimental measurement time is very short compared with the recurrence period.

### 3.2 Applications and prospects

Pendular states make accessible many stereodynamical properties. Studies of steric effects in inelastic collisions

or chemical reactions are a chief application. The use of a compact static electric field was exemplified by Loesch in a fine series of experiments [26]. The ability to turn the molecular orientation on or off enables modulation of angular distributions and other collision properties, thereby revealing anisotropic interactions not otherwise observable. Likewise, in photodissociation of oriented molecules, Miller has shown how pendular hybridization renders the laboratory photofragment distributions much more informative [33].

For all applications, the spectroscopy of pendular states has an important role, as the field dependence of suitable transitions reveals the extent of molecular orientation or alignment [27]. Conversely, the anisotropic distribution of the molecular axis imposes a corresponding anisotropy in the spatial distribution of transition moments, so alters the polarization of transmitted light. Slenczka has used this to develop a powerful form of polarization spectroscopy with dramatic resolution and sensitivity [34]. Moreover, because pendular hybridization is most effective for low rotational states, the spectra obtained for a room temperature gas become quite sparse, simplified to an extent otherwise attainable only by cooling to a few degrees Kelvin. Other features arising from the hybrid character of pendular states also prove valuable in spectroscopy, including the ability to tune transitions over a wide frequency range and to access states forbidden by the field-free selection rules [35]. Also, molecular alignment by an intense hybridizing field can greatly enhance transition intensities, so offers a means to improve markedly the sensitivity of chemical analysis by Raman spectroscopy [36].

In this "age of laser enlightenment", a host of notable experiments have produced molecular alignment by use of strong nonresonant laser pulses. In a seminal paper, Sakai with Stapelfeldt and colleagues at Århus gave the first experimental demonstration of the adiabatic alignment process [37]. Strong alignment was achieved for $I_2$ ($\langle \cos^2 \theta \rangle = 0.8$), and measured by imaging photodissociation fragments. The alignment and other properties of the process were found to agree nicely with the theory [28].

The Århus group extended the utility of this technique in several further experiments. It was shown that the branching ratio between different pathways for photodissociation of aligned molecules can be controlled by suitably selecting the laser polarization [38]. Another experiment showed the feasibility of aligning all three Euler angles of an asymmetric top molecule, by use of elliptically polarized alignment pulses [39]. Other studies demonstrated nonadiabatic alignment of an asymmetric rotor, using laser pulses much shorter than the molecular rotational periods to enable recurrence of the alignment after the molecules have entered a field-free region [40]. A fine review of both the theoretical and experimental status of molecular alignment by intense laser pulses has been presented by Stapelfeldt and Seideman [31]; this covers applications to high harmonic generation and nanoscale processing as well as to stereodynamics and control of reaction pathways.

The scheme depicted in Figure 2, combining a nonresonant pulsed laser field and a static electric field has thus far been implemented in only two experiments. Buck and colleagues applied the method as a diagnostic in interpreting anisotropy observed in photodissociation of the exotic molecule HXeI, an especially favorable case because both the dipole moment and polarizability of the molecule are exceptionally large [41]. Sakai and colleagues, at his home base in Tokyo, studied as a test case the orientation of OCS, a more typical molecule, and found results [42] in accord with the theory [30]. They also pointed out several prospective applications. Among these are stereodynamics of "dilute species such as highly-excited molecules or van der Waals clusters". Another is the possibility "to prepare selectively a single enantiomer from a 50–50% racemate sample", by orienting the sample using the combined-field technique together with an optimal, elliptically polarized laser pulse [43]. In this context, Sakai also suggests that by adding a static electric field, the method of aligning the three principal axes of an asymmetric rotor shown by the Århus group [39] can attain orientation, not just 3D alignment.

Orientation or alignment techniques combine happily with others in many ways. A few examples may suggest the wide range of prospects. If a molecule of interest is both polar and paramagnetic, the two-field scheme of Figure 2 can be modified by replacing the laser with a static magnetic field. Certain levels which in the magnetic field alone would be degenerate in energy will then be strongly split apart by the electric field, again in first-order fashion [44]. Other molecules may offer geometrical situations that permit "internal stereodynamics" to be probed. A striking instance is a study by Kong in which she makes use of an electric field to induce localization of a tunneling proton in gaseous tropolone between the two equivalent oxygen atoms [45]. Often, combining alignment with other techniques is mutually enabling. This was so in work of Yamanouchi and colleagues in Tokyo; they developed a pulsed gas electron diffraction apparatus and with it studied the alignment of $CS_2$ induced by intense nanosecond laser pulses, obtaining results that elucidated both the alignment process and the conditions required to get good diffraction patterns [46].

The ability to laser align molecules has contributed a key ingredient to a splendid new capability to probe what may be termed "electronic stereodynamics". In a remarkable development, tomographic imaging of the highest occupied molecular orbital of the $N_2$ molecule has been demonstrated by a consortium of Canadian researchers led by Corkum and in collaboration with Nilkura at PRESTO, Japan [47]. (The latter acronym, much used by magicians, now appears prescient!) In a lucid exposition of the imaging method [48], Stapelfeldt makes an analogy to medical tomography, wherein "the three-dimensional shape of a person's innards is derived from a series of two-dimensional X-ray images recorded at different angles". The new method uses laser pulses to create images for a series of molecular alignments, from which

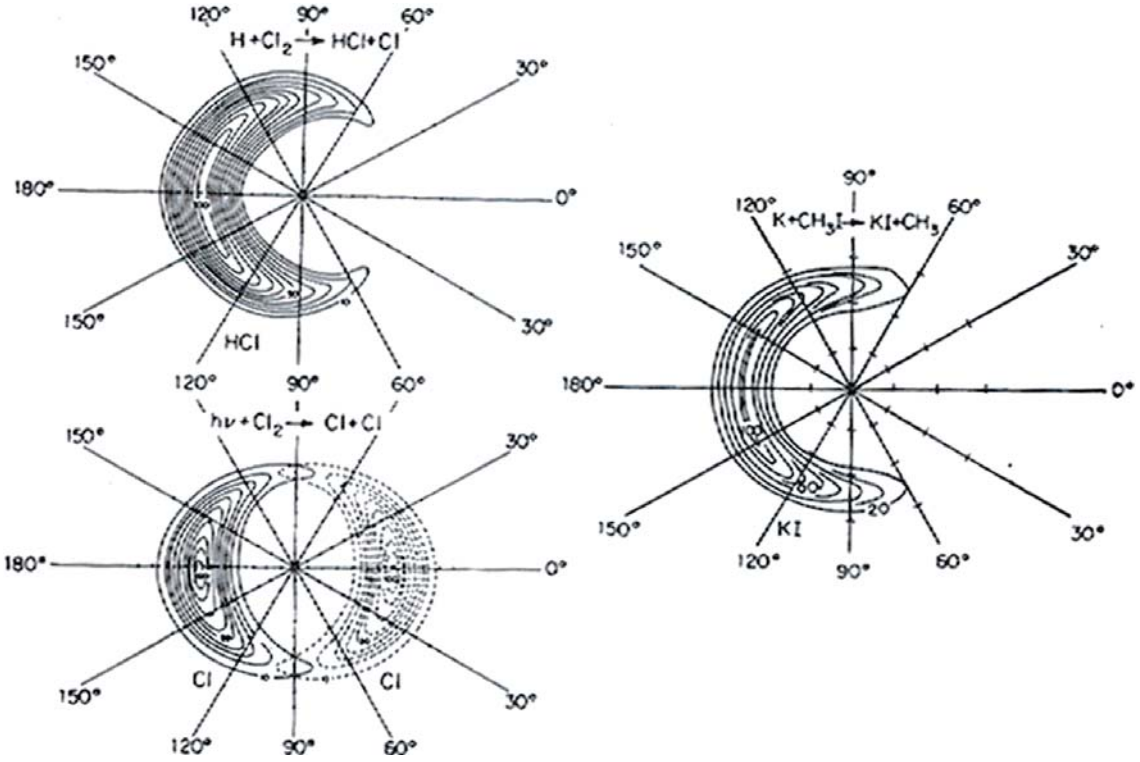


**Fig. 3.** Comparison of contour maps for photodissociation of the $Cl_2$ molecule and for reactive scattering of H + $Cl_2$ and K + $CH_3I$. Map for the latter case from work of Rulis and Bernstein [4]. For each map, origin is at center-of-mass and horizontal axis is along reactant relative velocity vector, with direction of incident atom or photon designated $\theta = 0°$. Tic marks along radial lines indicate velocity internals of 200 m/s.

computer tomography enables construction of the full three-dimensional shape of the electronic orbital.

This imaging method, deemed by its authors as "seemingly unlikely", emerged from extensive work on high-order harmonic generation, originally motivated as a unique source of coherent XUV radiation. High harmonics are generated by ionizing a molecule by an extremely intense and short laser pulse. The most loosely bound electron is ejected and accelerated away from the molecule by the strong electric field of the laser. A half-cycle later, that field reverses direction, bringing the electron back to collide with the parent molecule. The recollision process generates a wide range of overtones of the laser light; these high-harmonics often extend well beyond 50th order. Because the recolliding electron has gained much energy from the field of the ionizing laser, its wavelength becomes short enough to "probe the structure of the electron cloud through self-diffraction of the molecule" and thereby "the orbital structure is mapped onto the spectrum" of high-harmonics. The prealignment of the target molecule, previously found to strongly affect the efficiency of high harmonic production [49], and essential for tomography, was obtained using the now standard means to create pendular states via the polarizability interaction [31]. Prospects seem likely (in contrast to "seemingly unlikely"!) for extending such uncanny tomographic imaging to larger molecules, to excited electronic states, to study of any optically accessible orbital, and even to following electronic changes during chemical reactions [47].

## 4 Heuristic perspectives: frontier nodes and orbital asymmetry

In my view, the chief goal in developing experiments to elucidate single-collision reaction dynamics has been to advance understanding of how chemical kinetics is governed by electronic structure. Interpreting reaction dynamics in terms of electronic structure can now be greatly aided by ab initio computations. Yet it remains useful to invoke a rudimentary molecular orbital model. Many features of reaction dynamics can be explained by a few qualitative notions familiar from analysis of molecular geometry and spectra. The location of nodes and composition of the highest occupied orbital have key roles. This favorite theme is illustrated here with some venerable examples [50]. These have more than historical interest because the simple model proves widely applicable and suggests aspects that can be probed with new experimental methods.

Figure 3 displays angle-velocity contour maps revealing the striking kinship of the H + $Cl_2$ → HCl + Cl reaction to both photodissociation of $Cl_2$ and to the K + $CH_3I$ → KI + $CH_3$ reaction. For the H + $Cl_2$ reaction, the product angular distribution is broad but quite anisotropic,

with the HCl recoiling backwards and Cl forwards with respect to the incident H atom. The product velocity is very high, corresponding to release of about half of the reaction exoergicity into the translational recoil of HCl and Cl. The rest appears in vibrational and rotational excitation of HCl, observed in the infrared luminescence studied by Polanyi. The form of the angular distribution indicates collinear H–Cl–Cl as the preferred reaction geometry and the high recoil energy shows that strong repulsive forces are abruptly released.

The contour map for photodissociation corresponds to the continuous absorption spectrum of $Cl_2$, which shows directly the distribution of relative translational kinetic energy of the fragment Cl atoms and hence the repulsive energy release. The spectrum can be closely approximated by simply "reflecting" the Gaussian vibrational distribution of the ground electronic state from the steep ($\sim$7 eV/Å) repulsive wall of the dissociative excited electronic state. The angular distribution is governed by the dipole selection rule for absorption, which makes the transition probability vary as the square of the cosine of the angle between the Cl–Cl axis and the photon beam direction. Remarkably, H + $Cl_2$ and $h\nu$ + $Cl_2$ give similar angle-velocity contour maps. Indeed, the repulsive energy release is nearly identical, both in magnitude and in its Gaussian shape.

More remarkable still is the close resemblance of H + $Cl_2$ and K + $CH_3I$; except for a change of scale attributable to different exoergicity and mass ratios, the contour maps are almost congruent. In terms of electronic structure, a resemblance to photodissociation is obvious in the K + $CH_3I$ case, as the reaction involves transfer of the valence electron from K into the same strongly antibonding molecular orbital of I–$CH_3$ that is excited in photodissociation.

### 4.1 Role of frontier orbital node

In the H + $Cl_2$ case an analogy to photodissociation is not obvious, since the very high ionization potential of the H atom prohibits electron transfer. However, as indicated in Figure 4, the "frontier orbital" concept, fruitfully developed by Fukui, was found to provide a plausible rationale [50]. Collinear approach of H to $Cl_2$ generates three $\sigma$ orbitals for the H–Cl–Cl complex. The middle one of these, designated $2\sigma$, is the frontier orbital, the highest occupied orbital in the reaction complex. This orbital, which has one node along the internuclear axis, results from the superposition of two components, one H–Cl antibonding and Cl–Cl bonding, the other vice-versa. Simple semiempirical calculations indicate the latter component is quite dominant. Thus, the frontier node for the H atom reaction lies about midway between the chlorine atoms, just as in the antibonding sigma orbital of $Cl_2$, which when occupied induces photodissociation. This congruence in frontier nodes accounts for the strikingly similar repulsive energy release.

Other reactions of hydrogen atoms with halogen molecules provide instructive contrasts. As $Cl_2 \rightarrow Br_2 \rightarrow I_2$, the repulsive energy release becomes a smaller fraction

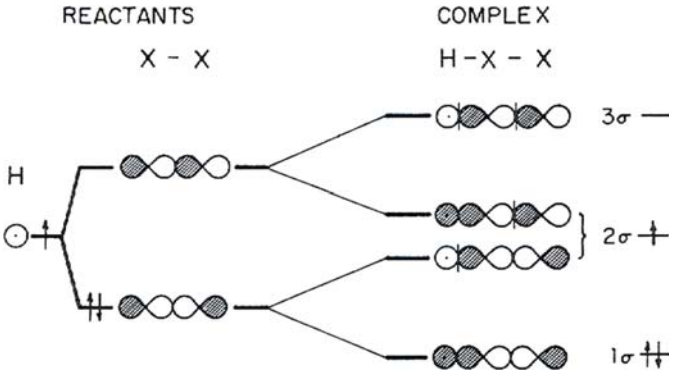


**Fig. 4.** Schematic construction of the three $\sigma$ molecular orbitals of collinear H–X–X. The frontier orbital, $2\sigma$, may be regarded as a superposition of two components, one H–X antibonding and X–X bonding, the other vice versa. Arrows indicate electron assignments.

of that in photodissociation, and the hydrogen halide angular distribution shifts from backwards to sideways with respect to the incident H atom direction. These trends are displayed in Figure 5. The molecular orbital model relates both trends to the decrease in halogen electronegativity. This enhances the $p$ character of hybrid orbitals involving the central atom and thereby favors a bent configuration for the reaction complex. The frontier node also shifts from midway between the halogen atoms in H–Cl–Cl to close to the central atom in H–I–I. Many analogous stable molecules are known that have one more or one less valence electron than these H–X–X systems. In accord with a molecular orbital treatment by Walsh [51], the molecules with one more electron are linear or nearly so; those with one less electron are strongly bent, with bond angles of 90° to 110°. Thus, it is plausible that the shift in location of the frontier orbital node with decreasing halogen electronegativity fosters bent reaction geometry as well as reducing the repulsive energy release.

### 4.2 Role of orbital asymmetry

For stereodynamics, reactions of the ICl molecule proved especially interesting. For instance, the H + ICl reaction is much more exoergic to form HCl (bond strength 120 kcal/mol) than to form HI (70 kcal/mol). Hence, on an energetic or statistical basis, reaction at the "Cl-end" would be more favorable than at the "I-end." That was the expectation of almost all chemists polled by me at seminars and meetings; indeed that opinion has persisted (even on three occasions this year), long after molecular beam and infrared chemiluminescence experiments demonstrated the contrary.

The molecular orbitals, shown in Figure 6, suggest that any reagent should prefer to attack at the I-end. As a consequence of the electronegativity difference, in ICl both the highest occupied orbital ($\pi^*$) and the lowest unoccupied orbital ($\sigma^*$) are predominantly composed of I atom orbitals, so reaction should at least be initiated at the

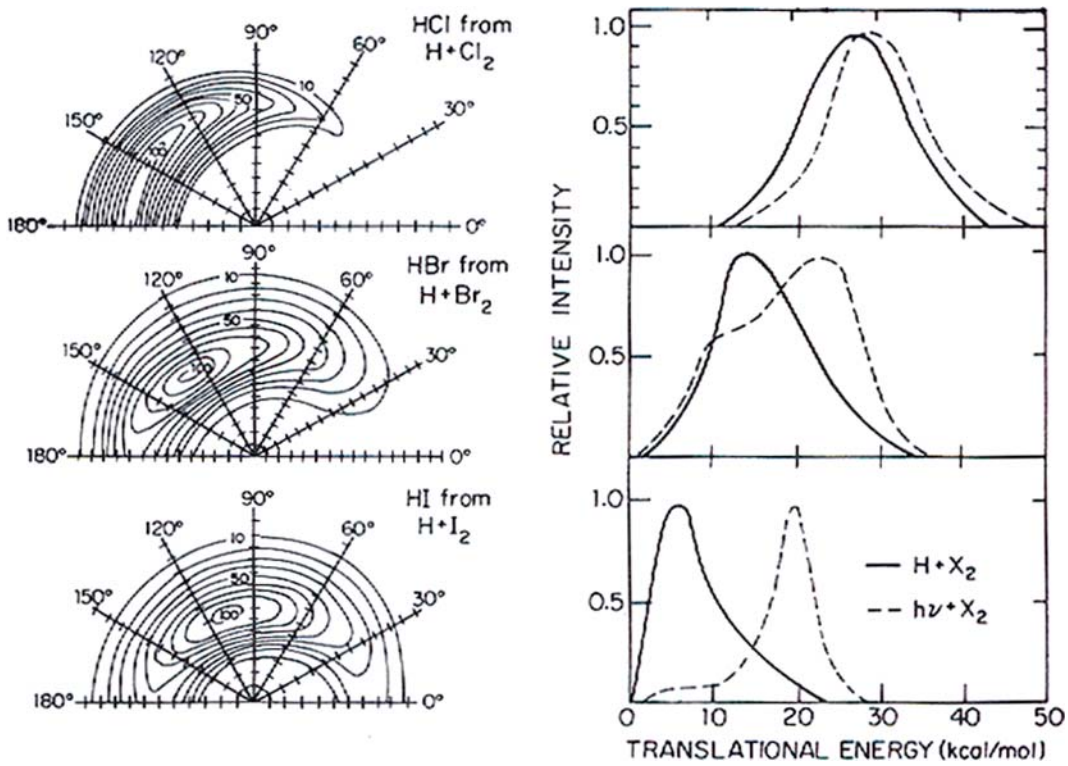


**Fig. 5.** Comparison of angle-velocity contour maps for reactions of H atoms with halogen molecules. Since maps must be symmetric with respect to the horizontal axis, only upper halves are shown. Tic marks along radial lines indicate velocity intervals of 200 m/s for $Cl_2$ case, 100 m/s for $Br_2$ And $I_2$. Panels at right compare distributions of product relative translational energy (solid curves) with continuous absorption spectra of halogen molecules (dashed curves). Abscissa scales for spectra are shifted to place origin at the dissociation asymptote, and thus show directly the repulsive energy release in photodissociation.

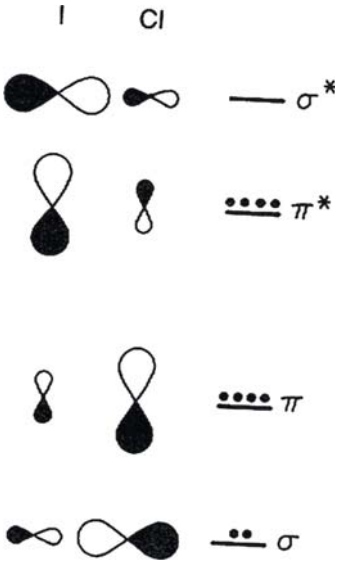


**Fig. 6.** Molecular orbitals for ICl, showing asymmetry resulting because the Cl atom is more electronegative than the I atom. Bonding orbitals $\sigma$ and $\pi$ are composed predominantly of Cl atomic orbitals, conjugate antibonding orbitals $\sigma^*$ and $\pi^*$ predominantly of I atomic orbitals. Dots indicate electron populations.

I-end. This orbital asymmetry accounts for several striking features of the spectra of interhalogen molecules, as Mulliken pointed out long ago.

Analogous steric preferences for many other atom transfer reactions can likewise be attributed to orbital asymmetry arising from differences in electronegativity. As seen in Figure 6, no matter whether the attacking reagent wants to remove or insert an electron, or some lesser partial charge, the target orbital involved favors the I-end of the ICl molecule. Indeed, beam studies found that as with H atoms, reactions of Br, O, and $CH_3$ with ICl all form predominantly iodides. This is remarkable, since these various reactions differ in many other ways. From analysis of triatomic molecular orbitals [5], there emerges a general criterion which might be termed the "electronegativity ordering rule". This predicts that H–X–Y will be a more favorable conformation than H–Y–X, if the X atom is less electronegative than Y (where these are any atoms with $p$ electrons). Likewise, in X–Y–Z systems, the preferred conformation has the least electronegative atom in the middle. The rule holds for almost all known stable triatomic molecules, linear or bent, and appears to apply also to preferred reactive conformations.

An especially telling example of the electronegativity ordering rule was found in reactions of O atoms with halogens. Whenever the O atom is more electronegative than one or both halogen atoms in the target molecule (i.e., Cl, Br, or I), the reaction goes readily, with no or very low activation energy. For mixed halogens XY with X less electronegative than Y (e.g., ICl or ClF), only the OX product appears and not OY, despite the much larger exoergicity for the latter path. This is nice evidence that the O atoms attacks end-on rather than inserting between the halogen atoms. However, since oxygen is less electronegative than

fluorine, the O + $F_2$ reaction should prefer the F–O–F geometry rather than O–F–F. This implies a relatively high activation energy, associated with the switch to an insertion mechanism, despite the large reaction exoergicity and the notorious chemical personalities of the reactants. In my informal polling of chemists, nobody believed this unorthodox prediction; all thought that O + $F_2$ would be at least as facile as the O + $Cl_2$ reaction. Subsequent experiments indeed confirmed that O + $F_2$ is inhibited by a large activation energy (∼12 kcal/mol); the rate at room temperature is about seven orders of magnitude slower than the O + $Cl_2$ reaction.

When the electronegativity difference between the attacking and target atoms becomes so large that electron transfer occurs, as often happens in reactions of alkali atoms, other instructive considerations enter. For instance, in the K + ICl reaction, the major product is KCl rather than KI. The key feature here is that the electron switch occurs at large distance (∼7 Å), so the actual reaction process involves a $K^+$ cation incident on an $(ICl)^-$ anion. Since the transferred electron must enter the $\sigma^*$ orbital of Figure 6, in the intermediate molecular anion this electron initially resides mainly on the I atom, but usually will shift to the more electronegative Cl atom as the $(ICl)^-$ anion dissociates in the strong field of the incoming $K^+$ cation. Auxiliary evidence supports this interpretation. For a variety of charge-transfer complexes with ICl, structure studies show that the donor group is adjacent to the I atom and the I–Cl bond distance is expanded, as expected when charge is deposited in the $\sigma^*$ orbital. The nonreactive scattering of alkali atoms from ICl shows distinctive features that indicate reaction is inhibited or precluded for an appreciable fraction of collisions at small impact parameters. These collisions may involve configurations in which the I (or $I^-$) atom blocks the access of K (or $K^+$) to the Cl atom.

Electronegativity differences also have a prominent role in reactions involving transfer of two atoms. In accord with the celebrated Woodward-Hoffmann rules, the favorite textbook reaction $H_2 + I_2 \rightarrow 2HI$ does not occur as an elementary process; instead it involves dissociation or near-dissociation of $I_2$ followed by I + $H_2$ + I. Many other four-center bimolecular reactions are likewise forbidden as concerted processes. However, when one or two of the atoms involved differ greatly in electronegativity, four-center reactions can become quite facile. Elsewhere, we have discussed such cases, including examples in which dramatic stereodynamic preferences are observed [52].

### 4.3 Inviting prospects

The several studies involving reactions with ICl noted here [50] were all done using randomly oriented molecules. Inferences about the stereodynamics were derived just from relative product yields and the form of angle-velocity contour maps, or for H + ICl, from a distinctive pattern of excitation of vibration and rotation in the HCl product. Clearly, much more incisive and definitive results could be obtained from experiments using oriented ICl molecules with state-of-the art laser spectroscopy and molecular beam methods. Indeed, ICl is well suited for the pendular orientation technique; it was one of the first molecules employed to demonstrate the method [27]. As yet, pendular orientation has been employed only in an exploratory study of K + ICl [26]. That reaction is atypical (as seen above) because it involves long-range electron transfer, which makes the process effectively a cation-anion dissociative recombination. In reactions with H, O, or halogen atoms, pendular orientation of the ICl would allow direct comparison of attack on the I-end or the the Cl-end.

As the new technique of tomographic imaging [47] preferentially selects the highest occupied molecular orbital, and operates at subfemtosecond time resolution, it appears ideally suited to following the evolution of the Fukui frontier orbital during a chemical reaction. In this regard, the reactions of alkali atoms or hydrogen atoms with halogens may serve as good candidates because, as indicated in Figure 3, for these the frontier orbital is expected to be singly occupied throughout the reaction. Photodissociation processes also appear particularly inviting for the tomographic imaging technique. For instance, HCN should be a good candidate as it is isoelectronic with $N_2$ and offers as well a large dipole moment.

## 5 Enzyme kinetics: new context for Langevin-Debye orientation

We who strive to elucidate the stereodynamics of small molecules in the gas-phase ought to be properly diffident when viewing the complexities presented by large biomolecules in solution. It is gratifying, however, to find that work on such systems often benefits from basic facts or concepts established in studies of small molecules. A celebrated example [53] is the stereospecific synthesis by Kishi of a neurotoxin molecule that has $2^{72}$ (i.e., $\sim 10^{21}$) stereoisomers. A key requisite for his strategic synthesis was knowledge of the conformational preference of an $sp^3$ carbon adjacent to an $sp^2$ carbon, found from the microwave spectrum of propylene. Here another biomolecular example is considered, involving conformational changes induced by enzyme action in catalyzing DNA replication. The Langevin-Debye formula for orientation of a dipole in an external field, which dates from 1913, has long been invoked in the "freely-jointed-chain" (FJC) model for polymer conformations. When modified to account for the restricted angular range allowed by interaction with the enzyme, this old formula proves useful in interpreting recent experiments observing the dependence on tension of the replication rate.

The experiments were done in the laboratories of Bustamante at Berkeley [54] and Bensimon [55] at Paris. A single DNA molecule, typically $10^4$ basepairs long, part single-stranded (*ss*) and part double-stranded (*ds*), is immersed in an ambient solution containing requisite nucleotides. A single enzyme molecule, spanning only ∼10 basepairs of the duplex and ∼4 *ss* bases of the

template, moves along the DNA, catalyzing addition of nucleotides to convert *ss* to *ds* segments. The replication rate is typically of the order of 100 base pairs/s. When tension is applied to the DNA by means of optical or magnetic "tweezer" techniques, the rate appears to increase modestly under low tension (up to ∼8 picoNewtons), then decreases markedly at higher tension (vanishing near ∼35 pN and reversing above). The strong dependence on tension indicates that the rate-determining step in the replication process involves work by the enzyme complex (and therefore motion) against the external force.

Interpretation of the experiments requires use of a model relating the replication rate to the tension-induced work. The original analysis [54,55] used data on the elasticity of *ss* and *ds* DNA, obtained from measurements in the absence of enzyme, to calibrate the amount of work involved in converting a single *ss* DNA base to *ds* geometry, thereby slightly shortening the template. This calibration was then assumed to apply as well in the presence of the enzyme. Accordingly, the activation barrier has no direct contribution from enzyme-DNA interactions; the only parameter having to do with the enzyme is $n$, the number of *ss* DNA bases converted to *ds* geometry in the transition state. Fitting this "global" model to the observed variations of replication rates with tension indicated, on the basis of the calibrated elasticity changes, shortenings that correspond to $n = 2$ for two of the enzymes studied and to $n = 4$ for a third enzyme. If correct, these results would have major implications concerning the replication and proofreading processes of DNA.

However, structural and bulk kinetic studies indicate that only one template base ($n = 1$) is converted from *ss* to *ds* during the rate-limiting conformational change of the enzyme-DNA complex. A likely source of the conflict with the interpretation of the tweezer results was the use of global extension vs. force curves for the entire polymer, with no reference to the enzyme-DNA complex. To examine this issue, Goel worked out a local, "structurally guided" model [56], in which the tension dependence of the activation energy is governed just by angular fluctuations of the two DNA segments neighboring the active site. The angular fluctuations were estimated by means of the FJC model, equivalent to using the Langevin-Debye formula with the field strength replaced by the tension force and the dipole moment replaced by the persistence length of the polymer. This version of a local model was chiefly heuristic. It required crude assumptions about the enzyme interactions, but served its intended purpose, showing that $n = 1$ could be consistent with the observed tension dependence.

By means of an extensive molecular dynamics simulation [57], done in collaboration with Andricioaei and Karplus, the local model was tested and enhanced. The simulation, based on crystal structure data and performed with the CHARMM program, treats explicitly the motion of 5,000 atoms and solvent water. The results confirmed the importance of angular motions of the DNA segments at the active site. The FJC model, which involves averaging orientations of the segments, weighted by a Boltzmann factor, was shown to be entirely inadequate. The chief amendment involves restrictions on the range of orientations allowed to the segments by the embrace of the enzyme. These steric restraints, incorporated by simply limiting the angular ranges in a modified Langevin-Debye formula, are the major factors determining the dependence on tension of the free energy of activation for the replication rate, in the range below 30 pN. At tensions above about 40 pN, the simulation revealed large conformational changes in the enzyme-bound DNA that may have a role in the experimentally observed tension-induced depolymerization. A major inference is that structurally imposed angular restraints likely will have a key role in many enzyme-catalyzed biomolecular reactions.

As a scientific meeting has a genetic function, serving to transmit seminal ideas and methods, this episode may offer an apt benediction for our conference.

It is a pleasure to thank Toshio Kasai and his colleagues for the opportunity to enjoy a conference so outstanding for considerate hospitality as well as scientific stimulation. In exploring stereodynamics, I am grateful to many able collaborators, particularly Bretislav Friedrich. My laboratory at Harvard has mainly been supported by the National Science Foundation and recently by the Department of Energy. This paper is dedicated to the memory of George Kwei (1939-2005); as a graduate student, he was the first to measure a two-vector correlation for a chemical reaction ($K + CH_3I$), 45 years ago.

## References

1. H. Tawara, *Pioneers of Physics in the Early Days of Japan* (North-Holland, 1989)
2. B. Friedrich, D. Herschbach, Phys. Today **56**, 53 (December, 2003)
3. D.S.Y. Hsu, G.M. McClelland, D.R. Herschbach, J. Chem. Phys. **61**, 4927 (1974)
4. D.R. Herschbach, Faraday Disc. Chem. Soc. **84**, 465 (1987)
5. D.R. Herschbach, in *The Chemical Bond*, edited by A. Zewail (Academic Press, New York, 1998), p. 175
6. D. Herschbach, in *Atomic and Molecular Beams*, edited by R. Campargue (Springer, Berlin, 2001), p. 3
7. L.C. Biedenharn, in *Nuclear Spectroscopy*, edited by F. Ajzenberg-Selove (Academic Press, New York, 1960), Part B, p. 732
8. D.A. Case, D.R. Herschbach, J. Chem. Phys. **64**, 4212 (1976)
9. D.A. Case, D.R. Herschbach, Mol. Phys. **30**, 1537 (1975); reprinted in Mol. Phys. **100**, 109 (2002)
10. G.M. McClelland, D.R. Herschbach, J. Phys. Chem. **83**, 1445 (1979)
11. J.D. Barnwell, J.G. Loeser, D.R. Herschbach, J. Phys. Chem. **87**, 2781 (1983)
12. D.A. Case, D.R. Herschbach, J. Chem. Phys. **69**, 150 (1978)
13. G.H. Kwei, D.R. Herschbach, J. Phys. Chem. **83**, 1550 (1979)
14. G.M. McClellandn, D.R. Herschbach, J. Phys. Chem. **91**, 5509 (1987)
15. S.K. Kim, D.R. Herschbach, Faraday Disc. Chem. Soc. **84**, 159 (1988)

16. M.H. Hijazi, J.C. Polanyi, Chem. Phys. **11**, 1 (1975)
17. R.B. Bernstein, D.R. Herschbach, R.D. Levine, J. Phys. Chem. **91**, 5365 (1987)
18. A.J. Orr-Ewing, W.R. Simpson, T.P. Rakitzis, S.A. Kandel, R.N. Zare, J. Chem. Phys. **106**, 5961 (1997); A.J. Orr-Ewing, W.R. Simpson, T.P. Rakitzis, S.A. Kandel, R.N. Zare **107**, 9382, 9392 (1997)
19. T.L.D. Collins, A.J. McCaffery, M.J. Wynn, Phys. Rev. Lett. **66**, 137 (1991); T.L.D. Collins, A.J. McCaffery, M.J. Wynn, Faraday Disc. **91**, 91 (1991)
20. M.D. Chen, K.L. Han, N.Q. Lou, Chem. Phys. Lett. **357**, 483 (2002)
21. M.P. de Miranda et al., J. Chem. Phys. **111**, 5368 (1999)
22. M.P. de Miranda, D.C. Clary, J.F. Castillo, D.E. Manolopoulos, J. Chem. Phys. **108**, 3142 (1998)
23. D.A. Case, G.M. McClelland, D.R. Herschbach, Mol. Phys. **35**, 541 (1978)
24. B. Friedrich, D.P. Pullman, D.R. Herschbach, J. Phys. Chem. **95**, 8118 (1991)
25. D.H. Parker, R.B. Bernstein, Ann. Rev. Phys. Chem. **40**, 561 (1989)
26. H.J. Loesch, Ann. Rev. Phys. Chem. **46**, 555 (1995)
27. B. Friedrich, D. Herschbach, Comm. At. Mol. Phys. **32**, 47 (1995); B. Friedrich, D. Herschbach, Int. Rev. Phys. Chem. **15**, 325 (1996)
28. B. Friedrich, D. Herschbach, Phys. Rev. Lett. **74**, 4623 (1995); B. Friedrich, D. Herschbach, J. Phys. Chem. **99**, 15686 (1995)
29. B. Friedrich, D. Herschbach, Z. Phys. D **36**, 221 (1996)
30. B. Friedrich, D. Herschbach, J. Phys. Chem. A **103**, 10280 (1999)
31. H. Stapelfeldt, T. Seideman, Rev. Mod. Phys. **75**, 543 (2003)
32. L. Cai, J. Marango, B. Friedrich, Phys. Rev. Lett. **86**, 775 (2001)
33. D.T. Moore, L. Oudejans, R.E. Miller, J. Chem. Phys. **110**, 197 (1999)
34. A. Slenczka, J. Phys. Chem. A **101**, 7657 (1997); A. Slenczka, Phys. Rev. Lett. **80**, 2566 (1998); A. Slenczka, Chem. Eur. J. **5**, 1006 (1999)
35. B. Friedrich, D. Herschbach, J.-M. Rost, H-G. Rubahn, M. Renger, M. Verbeek, J. Chem. Soc. Faraday Trans. **89**, 1539 (1993)
36. B. Friedrich, D. Herschbach, Chem. Phys. Lett. **262**, 41 (1996)
37. H. Sakai, C.P. Safvan, J.J. Larsen, K.M. Hilligsoe, K. Hald, H. Stapelfeldt, J. Chem. Phys. **110**, 10235 (1999); J.J. Larsen, H. Sakai, C.P. Safvan, I. Wendt-Larsen, H. Stapelfeldt, J. Chem. Phys. **111**, 7774 (1999)
38. J.J. Larsen, I.W. Wendt-Larsen, H. Stapelfeldt, Phys. Rev. Lett. **893**, 1123 (1999); M.D. Poulsen, E. Skovsen, H. Stapelfeldt, J. Chem. Phys. **117**, 2097 (2002)
39. J.J. Larsen, K. Hald, N. Bjerre, H. Stapelfeldt, Phys. Rev. Lett. **85**, 2470 (2000)
40. M.D Poulsen, E. Peronne, H. Stapelfeldt, C.Z. Bisgaard, S.S. Viftrup, E. Hamilton, T. Seiderman, J. Chem. Phys. **121**, 792 (2004)
41. N.H. Nahler, R. Baumfalk, U. Buck, Z. Bihary, R.B. Gerber, B. Friedrich, J. Chem. Phys. **119**, 224 (2003)
42. H. Sakai, S. Minemoto, H. Nanjo, H. Tanji, T. Suzuki, Phys. Rev. Lett. **90**, 083001 (2003); H. Sakai, S. Minemoto, H. Nanjo, H. Tanji, T. Suzuki, J. Chem. Phys. **118**, 4052 (2003)
43. K. Hoki, Y. Ohtsuki, Y. Fujimura, J. Chem. Phys. **114**, 1575 (2001)
44. B. Friedrich, D. Herschbach, Phys. Chem. Chem. Phys. **2**, 419 (2000); A. Boca, B. Friedrich, J. Chem. Phys. **112**, 3609 (2000)
45. C. Wu, Y. He, W. Kong, J. Chem. Phys. **121**, 4577 (2004)
46. K. Hoshina, K. Yamanouchi, T. Ohshima, Y. Ose, H. Todokoro, J. Chem. Phys. **118**, 6211 (2003)
47. J. Itatani, J. Levesque, D. Zeidler, H. Nilkura, J.C. Kleffer, P.B. Corkum, D.M. Villeneuve, Nature **432**, 867 (2004)
48. H. Stapelfeldt, Nature **432**, 809 (2004)
49. N. Hay, R. Velotta, M. Lein, R. de Nalda, E. Heesel, M. Castillejo, J.P. Marangos, Phys. Rev. A **65**, 053805 (2002); R. de Nalda, E. Hessel, M. Lein, N. Hay, R. Velotta, E. Springate, M. Castillejo, J.P. Marangos, Phys. Rev. A **69**, 031804(R) (2004)
50. D.R. Herschbach, Angew. Chem. Intl. Ed. Engl. **26**, 1221 (1987); see also reference [5]
51. A.D. Walsh, J. Chem. Soc. **1953**, 2260 (1953); A.D. Walsh, Disc. Faraday Soc. **35**, 223 (1963)
52. D.J. King, D.R. Herschbach, Faraday Disc. Chem. Soc. **55**, 331 (1973)
53. D.R. Herschbach, Phys. Today **50**, 11 (April, 1997)
54. G.J.L. Wuite, S.B. Smith, M. Young, D. Keller, C. Bustamante, Nature **404**, 103 (2000)
55. B. Maier, D. Bensimon, V. Croquette, Proc. Natl. Acad. Sci. USA **97**, 12002 (2000)
56. A. Goel, M.D. Frank-Kamenetskii, T. Ellenberger, D. Herschbach, Proc. Natl. Acad. Sci. USA **98**, 8485 (2001)
57. I. Andricioaei, A. Goel, D. Herschbach, M. Karplus, Biophys. J. **87**, 1478 (2004)